THE JOURNAL OF PHYSICAL CHEMISTRY B

Article

pubs.acs.org/JPCB

Disruption of Phosphatidylcholine Monolayers and Bilayers by Perfluorobutane Sulfonate

E. Davis Oldham,[†] Wei Xie,[†] Amir M. Farnoud,[‡] Jennifer Fiegel,[‡,§] and Hans-Joachim Lehmler*[,†,∥]

[†]Department of Occupational and Environmental Health, College of Public Health, University of Iowa, Iowa City, Iowa 52242, United States

[‡]Department of Chemical and Biochemical Engineering, College of Engineering, University of Iowa, Iowa City, Iowa 52242, United States

[§]Department of Pharmaceutical Sciences and Experimental Therapeutics, College of Pharmacy, University of Iowa, Iowa City, Iowa 52242, United States

[∥]Interdisciplinary Graduate Program in Human Toxicology, University of Iowa, Iowa City, Iowa 52242, United States

ABSTRACT: Perfluoroalkyl acids (PFAAs) are persistent environmental contaminants resistant to biological and chemical degradation due to the presence of carbon−fluorine bonds. These compounds exhibit developmental toxicity in vitro and in vivo. The mechanisms of toxicity may involve partitioning into lipid bilayers. We investigated the interaction between perfluorobutane sulfonate (PFBS), an emerging PFAA, and model phosphatidylcholine (PC) lipid assemblies (i.e., dimyristoyl-, dipalmitoyl- and distearoylphosphatidylcholine) using fluorescence anisotropy and Langmuir monolayer techniques. PFBS decreased the transition temperature and transition width of PC bilayers. The apparent membrane partition coefficients ranged from 4.9×10^2 to 8.2×10^2. The effects on each PC were comparable. The limiting molecular area of PC monolayers increased, and the surface pressure at collapse decreased in a concentration-dependent manner. The compressibility of all three PCs was decreased by PFBS. In summary, PFBS disrupted different model lipid assemblies, indicating potential for PFBS to be a human toxicant. However, the effects of PFBS are not as pronounced as those seen with longer chain PFAAs.

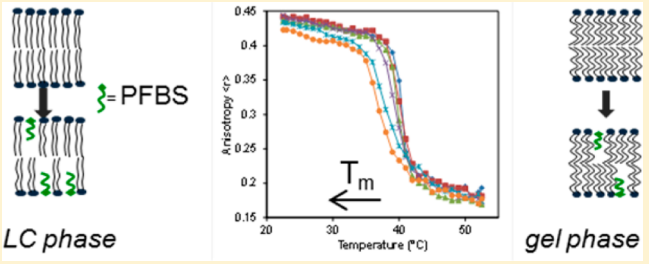

INTRODUCTION

Perfluoroalkyl acids (PFAAs) represent an emerging class of persistent organic pollutants in the environment. Large quantites of perfluorinated compounds, in particular, perfluoroalkyl sulfonamides, were produced industrially from perfluorooctanesulfonyl fluoride (POSF) for a wide range of purposes, including stain-repellant fabrics, lubricants, surfactants, and fire-fighting materials.[1] The perfluorinated chain of POSF-based chemicals, like other perfluorinated compounds, renders the compound resistant to chemical and biological degradation; furthermore, the perfluoroalkyl chain is both hydrophobic and lipophobic.[2] The polar headgroup of PFAAs and perfluorosulfonamides confers excellent surfactant properties. The perfluoroalkyl sulfonamides are metabolized to the corresponding sulfonates either in the environment or in animals.[3,4] These compounds are bioaccumulative and have been detected in water,[5] soil,[6] animals,[7] and humans.[8−10] Understanding the toxicity of PFAAs remains an important issue because of their widespread use and persistence.

Many PFAAs exhibit toxicity in humans and other animals. Several of these compounds are shown in Figure 1A. In particular, perfluorooctane sulfonate (PFOS) has been shown to display developmental toxicity. Decreased survival rates, birth rates, and delayed sexual maturation were observed in rats, mice, and monkeys exposed to PFOS.[11,12] Some studies suggest that PFOS interacts with peroxisome proliferator-activated receptor (PPAR).[13,14] We have previously suggested that neonatal mortality caused by PFOS may result from its partitioning into lipid assemblies,[15−17] which is consistent with previous studies.[18,19] Due to their toxicity and environmental concern, the use of perfluorooctanesulfonyl chemicals was replaced by the shorter perfluorobutanesulfonyl-based chemicals;[20] the main degradation product is perfluorobutane sulfonate (PFBS). The decreased length of the perfluoroalkyl chain was proposed to increase elimination rates and decrease bioaccumulation.[20,21]

Limited information is available regarding the toxicity of PFBS. In undifferentiated PC12 cells at 24 h, PFBS did not affect DNA synthesis or lipid peroxidation at any concentration investigated.[22] After 4 days of PFBS exposure, an increase in lipid peroxidation was seen. In contrast, PFOS and perfluorooctanoate (PFOA) decreased DNA synthesis and increased lipid peroxidation. Inhibition of gap junction communication in liver and kidney cells was not seen with PFBS;[23] the EC_{50} values for PFOS and perfluorohexane sulfonate (PFHS) in the same assay were 30 μM and 37 μM, respectively. The lowest

Received: May 7, 2012
Revised: July 23, 2012
Published: July 26, 2012

   dx.doi.org/10.1021/jp304412p | J. Phys. Chem. B 2012, 116, 9999−10007

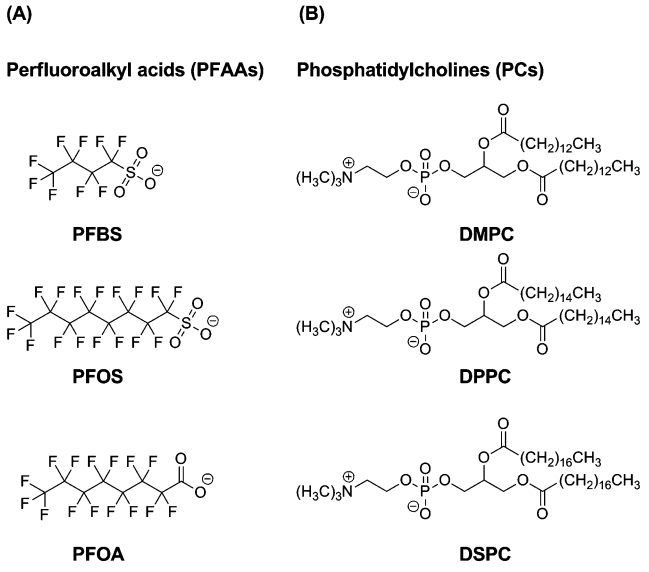

Figure 1. Chemical structures of (A) selected PFAAs and (B) phosphatidylcholines.

observable effect level (LOEL) for PFBS in a transactivation assay was 150 μM for murine PPARα and 30 μM for human PPARα. The corresponding LOELs for PFOS were 90 μM and 30 μM, respectively.

Very few in vivo toxicity studies of PFBS have been performed. The 3M Company conducted a two-generation study of PFBS toxicity in rats, and found no reproductive toxicity.[24] The doses of PFBS ranged from 30 to 1000 mg/kg body weight/day. By contrast, PFOS caused reproductive toxicity[25] and developmental neurotoxicity[26] in rats at a 3.2 and 3 mg/kg body weight/day, respectively. The half-life of PFBS was reported to be 4.7 h in male rats, 7.42 h in female rats, 95 h in male monkeys, 83 h in female monkeys, and 13−46 days in humans by the 3M Company;[21] in contrast, PFOS had a half-life of 7 days in male rats,[27] 110 or 130 days in monkeys (females or males, respectively),[28] and 1751 days in humans.[29] The shorter half-life for PFBS compared to PFOS is likely due to its lower affinity for serum albumin, which facilitates urinary excretion of PFBS.[30−32]

In this study we investigated the partitioning of PFBS into model lipid assemblies using fluorescence anisotropy and Langmuir monolayer studies. We used phosphatidylcholines (PCs) of varying chain lengths (Figure 1B) as models for lipid bilayers and pulmonary surfactant. As PFBS has been suggested to be less toxic than PFOS, we proposed that this decreased toxicity is a result of decreased lipid assembly partitioning.

EXPERIMENTAL METHODS

Chemicals. 1,2-Dimyristoyl-*sn*-glycero-3-phosphocholine (DMPC), 1,2-dipalmitoyl-*sn*-glycero-3-phosphocholine (DPPC), and 1,2-distearoyl-*sn*-glycero-3-phosphocholine (DSPC) were purchased from Avanti Polar Lipid (Alabaster, AL, USA). The structures are shown in Figure 1B. PFBS was obtained as the potassium salt from Fluka (Buchs, Switzerland, Lot# 396293/1). 1,6-Diphenyl-1,3,5-hexatriene (DPH) and 1-(4-trimethylammoniumphenyl)-6-phenyl-1,3,5-hexatriene (TMA-DPH) were obtained from Molecular Probes (Eugene, OR, USA). Tetrahydrofuran (THF), ethanol, chloroform, hexanes and 2-propanol were purchased from Fisher Scientific (Pittsburgh, PA, USA) and were HPLC grade. Purified water was obtained from a Milli-Q system at a resistivity greater than 18 MΩ·cm.

Fluorescence Anisotropy Measurements. Phospholipids (1 mL, 1 mM solution in chloroform) and fluorophore (2 μL, 1 mM in THF) were combined, concentrated, and dried under high vacuum. The resulting phospholipid−fluorophore films were then hydrated with 1 mL purified water for 1 h above the melting temperature of the respective phospholipid.[33,34] Large unilamellar vesicle (LUV) suspensions were obtained by extruding the MLV suspensions ~15 times through a double-stacked polycarbonate membrane filter (pore size: 200 nm) using a LiposoFast extruder (Avestin Inc., British Columbia, Canada) above the melting temperature of the respective phospholipid. The LUV suspensions were diluted 100-fold with an aqueous solution of PFBS to give final PFBS concentrations of 0 to 12 mM. Fluorescence anisotropy measurements were performed using a LS55 Luminescence Spectrometer from PerkinElmer (Shelton, CT, USA). The temperature was controlled with a Fisher Scientific Isotemp 3016D (Pittsburgh, PA, USA). The excitation and emission wavelengths were 350 and 452 nm, respectively.[35,36] Both the excitation and emission slit-widths were 10 nm.

The LUV solutions were equilibrated at temperatures of 40 °C (DMPC), 52.5 °C (DPPC) or 67.5 °C (DSPC). After 15 min, the samples were cooled to 10 °C (DMPC), 22.5 °C (DPPC) or 37.5 °C (DSPC) at a rate of 0.2°/minute with stirring. The temperature of the main fluid−gel phase transition (T_m), the transition width (ΔT_w), and the onset and offset of the transition were determined from plots of absolute fluorescence anisotropy ($\langle r \rangle$) as a function of temperature. The apparent partition coefficient K of PFBS between the lipids bilayers and the bulk aqueous phase was estimated using eq 1:[18,19]

$$-\Delta T_m = \frac{RT_{m,o}^2}{\Delta H_m}\left(\frac{K}{55.5 + C_L K}\right)C_S, \quad (1)$$

where ΔT_m is the change in melting temperature upon addition of PFBS, R is the gas constant, $T_{m,o}$ is the melting temperature of hydrated lipids, ΔH_m is the phase transition enthalpy (22.78, 36.59, and 44.46 kJ/mol for DMPC, DPPC, and DSPC, respectively),[37] C_s is the PFBS concentration, and C_L is the lipid concentration (10^{-5} M).

Monolayer Studies at the Air−Water Interface. All experiments were performed on a Langmuir−Blodgett apparatus (Minitrough System 4, KSV Instruments Ltd., Finland) with a Teflon-coated trough (782 × 75 × 5 mm) and two hydrophilic Delrin barriers that were compressed symmetrically. The surface pressure was measured by the Wilhelmy plate method using a platinum plate (perimeter: 39.24 mm; height 10 mm). The subphase consisted of 150 mM NaCl, 1.5 mM $CaCl_2$ dihydrate, and PFBS (0, 0.1, 1.0, or 10 mM) in purified water. After pouring of the subphase, the trough was heated to 37 °C and equilibrated for 15 min. The barriers were compressed, and surface-active impurities were removed from the air−water interface with a vacuum. The lipids (50 μL of a 1.662 mM solution in hexanes: 2-propanol = 9:1, v/v) were slowly spread over the subphase. The solvents were allowed to evaporate before the barriers were compressed at a constant speed of 10 mm/min (7.5 cm^2/min). Limiting molecular areas were calculated by extrapolating the linear region of the isotherm in the solid phase to zero surface pressure.

dx.doi.org/10.1021/jp304412p | J. Phys. Chem. B 2012, 116, 9999−10007

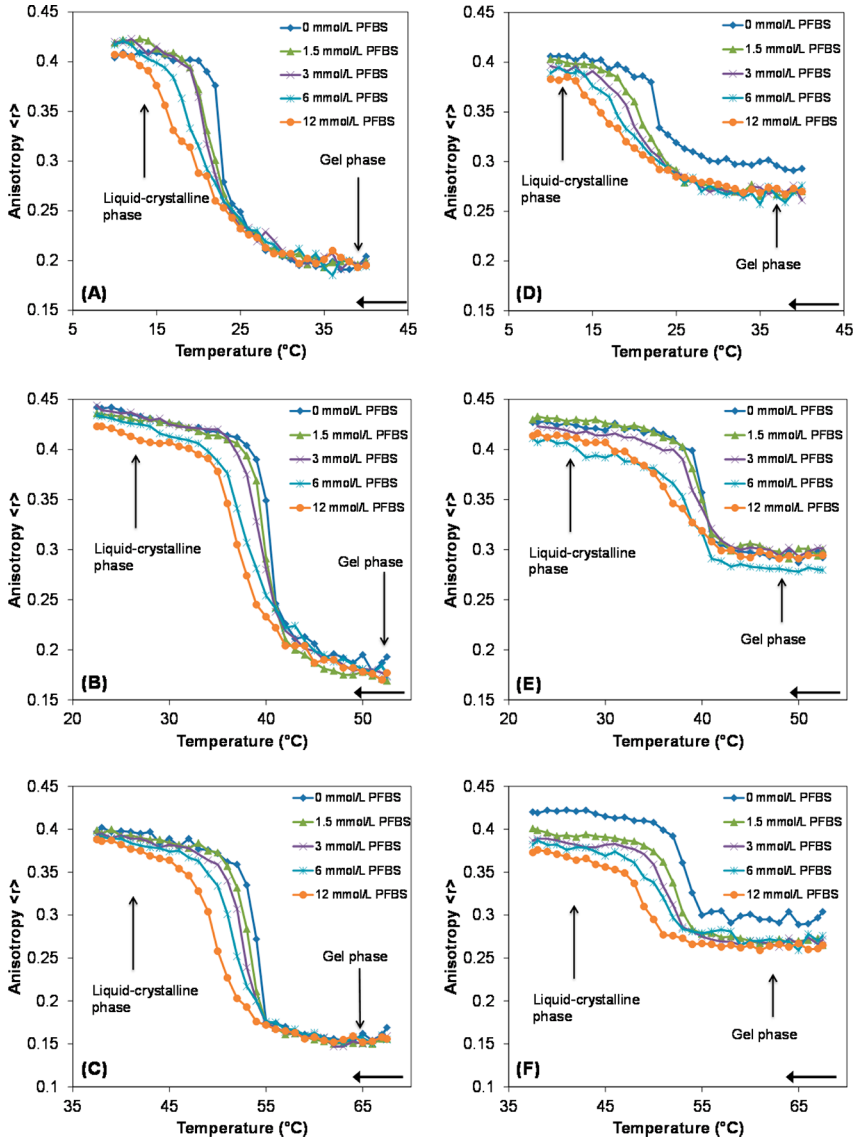

Figure 2. Fluorescence anisotropy as a function of temperature for PC−PFBS mixtures. Representative plots from at least three experiments are shown. The liquid-crystalline and gel phases are indicated by arrows. DPH was used as the probe for (A) DMPC−PFBS, (B) DPPC−PFBS, and (C) DSPC−PFBS. TMA-DPH was used as the probe for (D) DMPC−PFBS, (E) DPPC−PFBS, and (F) DSPC−PFBS. The samples were cooled at a rate of 0.2 °C/min, as indicated by the arrows.

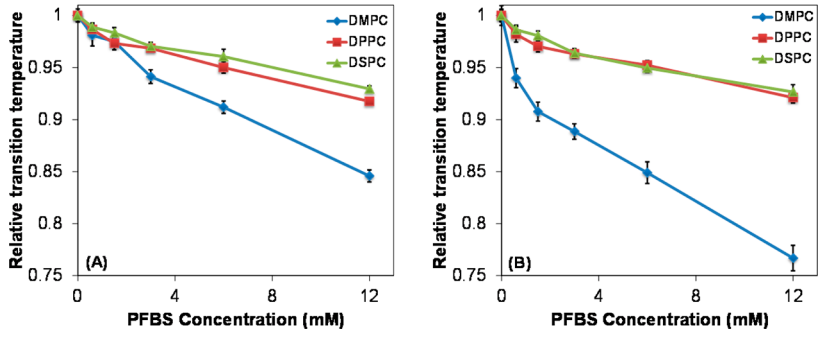

Figure 3. Decrease in T_m of PCs as a function of PFBS concentration. Relative melting temperature is defined as $T_m/T_{m,o}$, with (A) DPH and (B) TMA-DPH as the fluorophores.

RESULTS

Fluorescence Anisotropy. The ability of PFBS to partition into DMPC, DPPC, and DSPC bilayers was measured using fluorescence anisotropy. The fluorophores DPH and TMA-DPH were used as previously described.[15−17] These fluorophores were chosen because their position within lipid bilayers has been well characterized. DPH positions itself closer to the middle of the bilayer than TMA-DPH.[38] Thus

dx.doi.org/10.1021/jp304412p | J. Phys. Chem. B 2012, 116, 9999−10007

differences in the fluorescence anisotropy between DPH and TMA-DPH vesicles are indicative of the location of PFBS in the lipid bilayer. The plots of fluorescence anisotropy versus temperature are shown in Figure 2. PFBS had concentration-dependent effects on the transition temperature (T_m), the width of the transition, and the magnitude of fluorescence anisotropy, a measure of lipid bilayer fluidity, in both the liquid-crystalline and gel phases of all three PCs.

Fluorescence anisotropies of all three PCs in the gel phase and liquid-crystalline phase changed, depending on the PFBS concentration and fluorophore employed, indicating changes in bilayer fluidity. In the liquid-crystalline phase, PFBS caused concentration-dependent increases in fluidity for all three PCs with both fluorophores (Figure 2). The gel phase was less sensitive to the addition of PFBS with DPH as fluorophore (Figure 2A–C), as only DPPC showed a small change in fluidity in this phase (Figure 2B). In contrast fluidity increased to a greater extent for all three PCs when the fluorophore was changed to TMA-DPH (Figure 2D-F). In the liquid-crystalline phase pronounced fluidity increases were observed for each of the PCs, with the greatest change occurring for DSPC (Figure 2F). In contrast to experiments with DPH as fluorophore, increases in fluidity were observed in the gel phase for all the PCs with TMA-DPH as fluorophore.

The T_m values, normalized to the T_m of the pure phospholipids, as a function of PFBS concentration are shown in Figure 3. With both DPH and TMA-DPH as the fluorophore, all three PCs showed a reduction in T_m with increasing concentrations of PFBS. The relative reductions in T_m of DSPC and DPPC were comparable. At PFBS concentrations of 3 mM or greater, the relative reduction in melting temperature for DMPC was greater than for DPPC and DSPC, with DPH as the fluorophore. With TMA-DPH, the relative decrease in T_m was greater for DMPC than DPPC and DSPC, which were comparable with each other. Thus the reduction in T_m did not show a clear dependence on PC chain length. The absolute change in T_m was used to calculate apparent partition coefficients for PFBS for each lipid, according to eq 1; these results are summarized in Table 1.

Table 1. Partition Coefficients for PFBS and PCs[a]

Lipid	K(DPH) × 10^2	K(TMA-DPH) × 10^2
DMPC	4.9	6.6
DPPC	6.6	5.7
DSPC	8.2	8.5

[a]The values were determined from eq 1.

The apparent partition coefficients were comparable and ranged from 4.9 × 10^2 to 8.5 × 10^2; with either probe, the apparent partition coefficient observed for DSPC tended to be larger compared to DMPC or DPPC.

The width of the liquid-to-gel transition, a measure of the cooperativity of the lipid bilayer, was also affected by PFBS concentration. The magnitude of this effect varied between the three PCs, as shown in Figure 4. With DPH as the fluorophore, all three PCs showed similar transition widths up to 3 mM; at higher concentrations, DMPC exhibited a broader transition than DPPC and DSPC. When TMA-DPH was used, the transition width for DMPC was greater than DMPC and DSPC at concentrations of 1.5 mM or higher. The widths for DMPC and DSPC were comparable at PFBS concentrations up to 3 mM. At 6 mM PFBS, the rank order of the transition width was DMPC > DPPC > DSPC.

Disruption of Phospholipid Monolayers at the Air–Water Interface. The effect of PFBS on the behavior of the three lipids was studied at the air–water interface. Compression isotherms were obtained on a subphase consisting of 150 mM NaCl, 1.5 mM $CaCl_2$ and increasing PFBS concentrations at 37 °C. These conditions have been used previously in studies of pulmonary surfactants, as they reflect ion concentrations found in alveoli.[39,40] Representative compression isotherms are shown in Figure 5. Changes in limiting molecular area, which represents the minimum surface area per molecule, area at collapse, and pressure at collapse, were determined from the average of three compression isotherms and are summarized in Table 2.

For DMPC, the shape of the isotherms was not affected by PFBS. At mean molecular areas of 110 Å^2/molecule, the surface pressure increased from <0.3 mN/m (no PFBS) to 7 mN/m (10 mM PFBS). The limiting molecular area, area at collapse, and pressure at collapse were also affected in a concentration-dependent manner. For example, the limiting molecular area increased from 75.3 Å^2/molecule for pure DMPC to 102 Å^2/molecule with 10 mM PFBS in the subphase. Likewise, the area at collapse increased from 48.3 Å^2/molecule to 57.9 Å^2/molecule, while the pressure at collapse decreased from 47.2 to 29.6 mN/m.

DPPC exhibits a liquid-expanded (LE) to liquid-condensed (LC) transition at approximately 55 Å^2/molecule. This transition was shifted toward a smaller molecular area with 0.1 mM PFBS in the subphase, and was completely eliminated at concentrations of 1 mM and 10 mM PFBS. As with DMPC, the limiting molecular area and area at collapse increased with increasing PFBS concentration, while the pressure at collapse decreased. At an area of 110 Å^2/molecule, the surface pressure

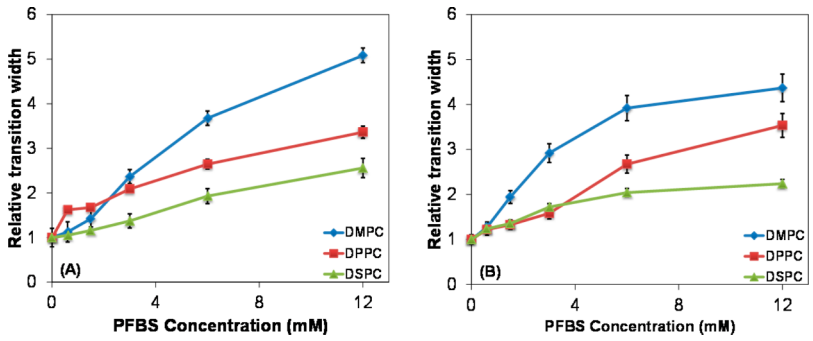

Figure 4. Relative phase transition widths for DMPC, DPPC, or DSPC with (A) DPH and (B) TMA-DPH as the fluorophore.

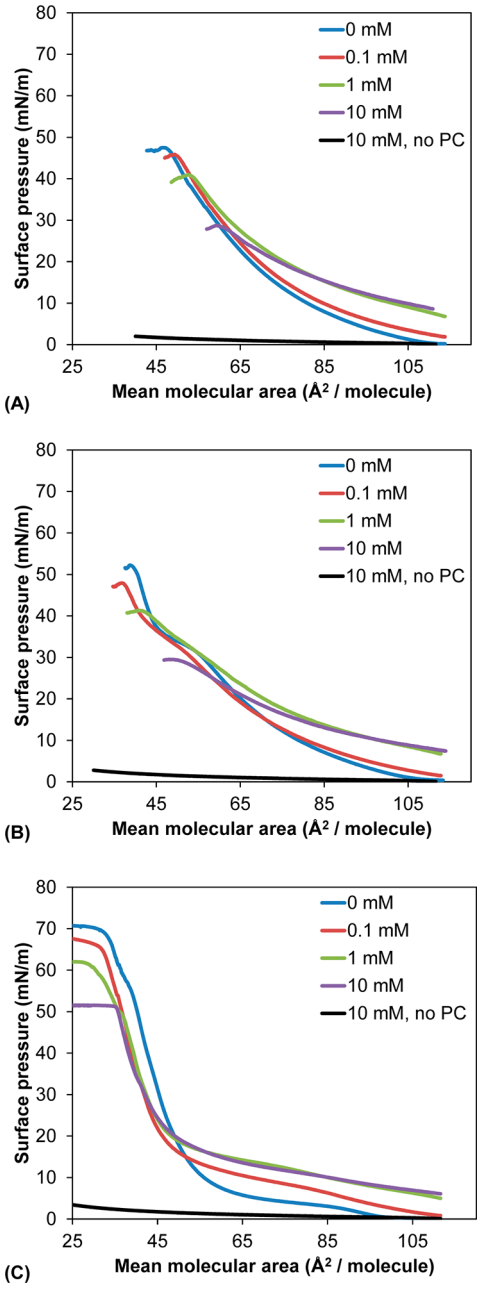

Figure 5. Representative compression isotherms (from three replicates) for (A) DMPC, (B) DPPC, and (C) DSPC in the presence of increasing concentrations of PFBS. The compression isotherms were obtained at 37 °C on a subphase consisting of 150 mM NaCl and 1.5 mM $CaCl_2$, with a compression rate of 10 mm/min (7.5 cm^2/min). PCs were added as a solution in 9:1 (v:v) hexanes:ethanol, which was allowed to evaporate before compression. The LE-to-LC transition for DPPC is shown with an arrow. Control isotherms were obtained by the addition of blank solvent to PFBS-containing subphases followed by compression. Only the control for the 10 mM PFBS subphase, which gave the highest surface pressure change upon compression, is shown on each graph.

increased from <0.3 mN/m in the absence of PFBS to 7 mN/m with 10 mM PFBS. The pressure at collapse decreased from 50.4 to 29.3 mN/m, the area at collapse increased from 37.1 to 48.5 $Å^2$/molecule, and the limiting molecular area increased from 59.1 $Å^2$/molecule to 94.1 $Å^2$/molecule over the same concentration range.

Pure DSPC underwent a transition to the liquid phase at 100 $Å^2$/molecule on the NaCl/$CaCl_2$ subphase. At 0.1 mM PFBS, this transition was eliminated. Unlike DMPC and DPPC, the area at collapse was comparable over the entire concentration range. The limiting molecular area decreased from 61.2 $Å^2$/molecule at 0 mM PFBS to 49.4 $Å^2$/molecule at 10 mM PFBS, which is also in contrast to DMPC and DPPC. The pressure at collapse did decrease from 69.1 to 51.3 mN/m over the range of 0 to 10 mN PFBS in the subphase. The surface pressure at 110 $Å^2$/molecule increased with increasing PFBS concentration, as seen with DMPC and DPPC.

The compressibility of the lipids was calculated from the compression isotherms; the compression moduli, smoothed for clarity, are shown in Figure 6. PFBS decreased the maximum compressibility of DMPC from 108 to 52 mN/m. The compression moduli of DPPC, in contrast to DMPC, were biphasic in the absence of PFBS due to the presence of LE and LC phases. Biphasic compressibility curves are known in the literature.[41] The broad peak at 30 $Å^2$/molecule corresponds to the LE phase, while the sharp peak at 50 $Å^2$ corresponds to the LC phase. With increasing PFBS concentration, this magnitude of this peak decreased, indicating the loss of the LC phase. At 10 mM PFBS the maximum compressibility was lowered to 47 mN/m. PFBS affected DSPC compressibility in a manner similar to that of DMPC. The maximum compressibility decreased from 210 mN/m at 0 mM PFBS in the suphase to 161 mN/m at 1 mM PFBS.

DISCUSSION

PFBS is an emerging persistent organic pollutant used to replace PFOS in a range of consumer and industrial applications.[20,21] This change was necessitated by the observation that PFOS is environmentally persistent and causes adverse reproductive health effects in rodents and humans.[11,12,42] The neonatal toxicity of PFOS is a particular concern[11,12] and may be a result of an interaction between PFOS and pulmonary surfactants. However, less is known about the adverse effects of PFBS. Because of its structural similarity to PFOS, PFBS is likely to partition into lipid assemblies and potentially cause toxicity by similar mechanisms. We investigated the interaction of PFBS with PC lipid assemblies, since DPPC is the major component of pulmonary surfactants. Furthermore, PC bilayers are frequently used as model membranes.

The toxicity of PFAAs may be explained in part by their partitioning between lipid assemblies and the bulk aqueous phase. PFOS[17] and PFOA[15] have been shown to readily partition into PC lipid assemblies using fluorescence anisotropy experiments. In these studies, the addition of PFAAs decreased the transition temperature of various PCs. The reduction in T_m results from the incorporation of the perfluorinated tails of PFAAs into lipid assemblies. From the reduction in T_m of the bilayer, the apparent partition coefficients of PFOS were calculated to be $4.4 - 8.8 \times 10^4$.[15] In the present study, the corresponding apparent partition coefficients for PFBS were 100-fold smaller and ranged from $4.9 - 8.5 \times 10^2$. These values are comparable to the coefficients for the longer-chain hydrocarbon surfactants octanoate and octanesulfonate.[16,18] The partition coefficient of PFBS was essentially independent of PC chain length, which has been seen previously with PFOS, PFOA, and fluorinated anesthetics.[15,17,43] This difference in membrane partitioning between PFOS and PFBS is, to some extent, consistent with previous work investigating the

dx.doi.org/10.1021/jp304412p | J. Phys. Chem. B 2012, 116, 9999−10007

Table 2. Parameters of PC Monolayers as a Function of PFBS Concentration[a]

lipid	concentration (mM)	limiting molecular area (Å²/molecule)	area at collapse (Å²/molecule)	pressure at collapse (mN/m)	maximum compressibility (mN/m)
DMPC	0	75.3 ± 2.5	48.3 ± 1.1	47.2 ± 0.2	107.7 ± 5.1
	0.1	78.0 ± 1.3	48.9 ± 0.6	46.0 ± 0.3	100.5 ± 1.7
	1	85.4 ± 1.0	51.8 ± 1.7	41.3 ± 0.3	81.9 ± 1.5
	10	102 ± 1	57.9 ± 1.6	29.6 ± 0.6	52.0 ± 1.6
DPPC	0	59.1 ± 2.2	37.1 ± 1.4	50.4 ± 1.3	102.7 ± 1.4
	0.1	61.0 ± 2.3	37.7 ± 0.9	48.1 ± 0.6	99.5 ± 8.2
	1	89.4 ± 1.4	40.5 ± 1.0	42.0 ± 0.6	60.4 ± 1.4
	10	94.1 ± 4.3	48.5 ± 0.8	29.3 ± 0.2	46.5 ± 2.6
DSPC	0	61.2 ± 4.8	27.0 ± 0.6	69.1 ± 0.9	210.1 ± 7.1
	0.1	51.0 ± 1.5	29.0 ± 1.6	66.7 ± 0.4	197.4 ± 10.1
	1	55.2 ± 3.8	25.9 ± 1.2	62.8 ± 1.1	160.2 ± 10.6
	10	49.4 ± 3.1	28.7 ± 2.5	51.3 ± 0.3	161.2 ± 11.6

[a]Limiting molecular area, area at collapse, collapse pressure, and maximum compressibility obtained from compression isotherms recorded using subphases containing different PFBS concentrations.

partitioning of fluorinated surfactants in biological and environmental systems. For example, Jones et al. found PFBS bound less to chicken or eagle serum proteins, as shown by displacement of corticosteroids, than PFOS.[32]

The width of the phase transition of the three PCs was also increased by addition of PFBS. At high concentrations (12 mM PFBS), the relative (Figure 4) and absolute transition widths increased in the order DSPC > DPPC > DMPC. Only a few other studies have systematically investigated the effect of persistent organic pollutants on model membranes containing PCs with different hydrophobic tails. PFOS[17] and PFOA[15] have been shown in fluorescence anisotropy and differential scanning calorimetry (DSC) studies to increase transition widths of PCs with a similar rank order at higher surfactant concentrations. Nonfluorinated small molecules, such as tamoxifen derivatives[44] and pyrethroid[45] pesticides, also showed the same order as the PFBS fluorescence experiments. Overall, the increase in transition width of DMPC, DPPC, and DSPC indicates a loss of cooperativity in PFBS-containing bilayers. The differences in the transition width between the three PCs under investigation are due to an increase in van der Waals forces between the hydrophobic tails as the PC chain length increases, resulting in an increase in cooperativity of the lipid bilayer and overall smaller transition width, with the observed rank order DMPC > DPPC > DSPC. The reduced cooperativity of DMPC bilayers compared to DPPC and DSPC also explains the more pronounced effect of PFBS on T_m of DMPC bilayers.

In addition to the effects on phase transition temperature and transition width, PFBS increased the fluidity of all three PCs investigated. In the liquid-crystalline phase and, with some exceptions (see Figure 2A,C), the gel phase, fluidity increased, as indicated by a decrease in fluorescence anisotropy upon addition of PFBS. In previous studies PFOS[17] and PFOA[15] increased membrane fluidity in the gel phase but decreased fluidity in the liquid-crystalline phase. PFOS also caused a concentration-dependent increase in cell membrane fluidity in HL-60 leukemia cells and alveolar macrophages.[17] Both the fluorescence anisotropy and in vitro cell culture experiments used 100 to 1000-fold lower concentrations than the PFBS concentrations used in this study. The decreased fluidizing effect of PFBS compared to PFOS and PFOA has also been seen in flow cytometry experiments.[46]

Taken together, our findings suggest that PFBS partitions into the lipid bilayer and, as indicated by its more pronounced effect on fluorescence anisotropy in the DPH-TMA experiments, is located near the lipid–water interface. Analogous to other anionic, small molecules, the sulfonate group most likely interacts with the positively charged trimethylammonium part of the PC headgroup,[47] and the perfluorobutyl chain is expected to align itself vertically with the hydrophobic tails within the lipid assemblies.[48,49] The disruption of lipid assemblies by PFBS results in the generation of free volumes in the interior of the lipid bilayer[47] (i.e., the chains of DPPC are twice as long as PFOS and four times as long as PFBS). To maximize van der Waals interactions within the hydrophobic core of the bilayer, the hydrophobic tails of the PCs undergo *trans–gauche* isomerization and incorporate chain bends; these changes disrupt the long-range order of the bilayer. In addition, Inoue and co-workers have proposed that the negatively charged head groups, such as sulfonate or carboxylate groups, repel each other, causing disruption of the packing within the lipid bilayer. This disruption results in a decrease of the transition temperature.

The combination of ionic interactions and free volumes not only explain the decrease in T_m but also the increase in the transition width and the increase in fluidity. PC bilayers consist of domains of similar size and shape, resulting in a sharp peak for the main phase transition of fully hydrated PCs.[50−52] Incorporation of PFBS can potentially reduce the size of domains and, as a result, increase the number of domains, thus causing a decrease in T_m and a broadening of the main phase transition. This may be due to preferential positioning of PFBS, similar to other small molecules, at the interface of these domains, resulting in more ramified domain borders. Furthermore, lateral phase separation into PFBS-poor and PFBS-rich domains may occur in PFBS-containing PC bilayers. This lateral phase separation can conceptually be compared to the bulk phase separation of fluorocarbons and hydrocarbon liquids[2] and the nonideality of mixing of micelles of fluorocarbon and hydrocarbon surfactants.[53]

In addition to studies with PC bilayers, analysis of PC monolayers at the air–water interface may provide important information about PFBS neonatal toxicity, as DPPC is the major component of pulmonary surfactant, and PFBS, like the structurally related PFOS,[54−56] may be present in amniotic fluid. Similar to model bilayers, PFBS also disrupted PC monolayers at the air–water interface. The limiting molecular area, maximum pressure, area at collapse, and compressibility

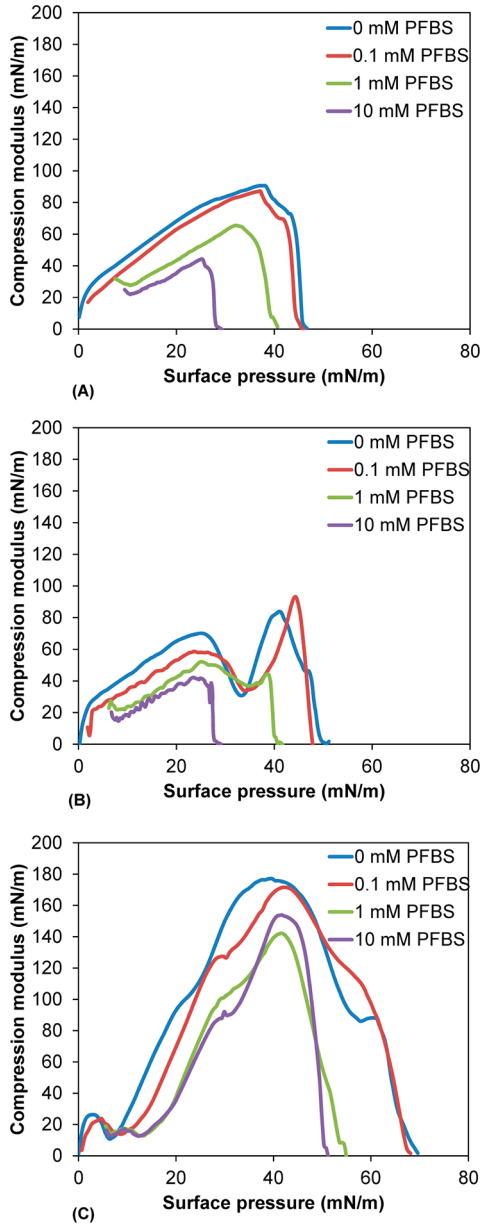

Figure 6. Compression modulus curves for (A) DMPC (B) DPPC and (C) DSPC in the presence of 0 mM PFBS (blue), 0.1 mM PFBS (red), 1 mM PFBS (green) and 10 mM PFBS (purple). Compression modulus is calculated as $-A(d\pi/dA)$. Each curve represents the average of three compression experiments.

were all affected by PFBS, which suggests that PFBS partitions into these PC monolayers and alters their behavior at the air–water interface. From a toxicological point of view, the decrease in maximum pressure is noteworthy because it indicates that PFBS inhibits the action of pulmonary surfactants, which can lead to alveolar collapse.

The increase in limiting molecular area for DMPC and DPPC is consistent with this interpretation as the presence of PFBS molecules in the monolayer is expected to increase the limiting molecular area. In contrast, DSPC showed a decrease in the limiting molecular area, which maybe be associated with the more solid-like character of DSPC-based monolayers. Specifically, only DSPC monolayers exhibited maximum compressibilities greater than 150 mN/m, a value that is considered to indicate a solid monolayer.[57] PFOS has been shown to partition more efficiently into DPPC in the LE state than in the LC state. DPPC and DMPC exist in a more expanded state under the conditions of this study, which may explain why PFBS more effectively increases the limiting molecular area of DPPC and DMPC monolayers compared to DSPC monolayers. The decrease in the limiting molecular area of PFBS-containing DSPC monolayers suggests that PFBS-DSPC interactions result in a more close packing. Indeed, there are reports that the anionic character of surfactant may influence the closeness of packing. Sodium dodecyl sulfate (SDS), for example, increases the order of the chains in neutral, zwitterionic DMPC monolayers,[58] but inhibits close packing in charged DMPG monolayers.[59] However, in-depth studies of the PFBS partitioning into PC monolayers and PFBS-PC interactions at the air–water interface are needed to confirm this hypothesis.

The interactions between phospholipids and PFOS and PFOA at the air–water interface have been previously described[48] and are comparable to the effects of PFBS on DPPC monolayers at reported in this study, although the concentrations of PFOS and PFOA used were 100-fold lower than those used for PFBS. DPPC monolayers exhibited a higher limiting molecular area in response to increasing PFOA or PFOS concentrations. For example, at 0.1 mM PFOS the limiting molecular area increased from 53.0 Å^2 for pure DPPC to 63.0 Å^2. The maximum compressibility decreased from 191.2 for pure DPPC to 145.9 mN/m with 0.1 mM PFOS in the subphase; PFOA caused a similar decrease in maximum compressibility. The LE/LC transition was eliminated with 0.01 mM PFOS or 0.1 mM PFOA, whereas 1 mM PFBS was required to abolish this transition. The compression studies with PFOS and PFOA were performed on a pure water subphase at 13 to 20 °C, so the results cannot be quantitatively compared to this study.

Similar to the fluorescence anisotropy experiments, 2 orders of magnitude higher concentrations of PFBS were necessary to elicit the changes seen with PFOS. This finding can be explained with differences in the equilibrium air–water interface partitioning reported for PFOS and PFBS. On the basis of published bulk water to air–water interface partitioning coefficients (1871 M^{-1} for PFOS and 40.4 M^{-1} for PFBS[60]), the number of PFBS molecules at the air–water interface increases approximately 10- and 72-fold when increasing the PFBS concentration from 0.1 to 1 and 10 mM, respectively. A much lower bulk solution concentrations of PFOS are needed to obtain similar numbers of PFOS molecules at the air–water interface. For example, the number of PFOS molecules at 0.1 mM, the highest PFOS concentration used in the study by Matyszewska et al.,[48] is estimated to be comparable to the number of PFBS molecules at the air–water interface at 10 mM in the present study. In other words, in the concentration ranges investigated 2 orders of magnitude higher bulk concentrations of PFBS are needed to achieve a similar number of PFBS and PFOS molecules at the air–water interface and, thus, cause a comparable effect of PC monolayers at the air–water interface.

■ CONCLUSION

In this work, we measured the ability of PFBS to partition into various lipid assemblies as models for cell membranes. PFBS effectively partitioned into lipid bilayers and monolayers consisting of PCs, the major component of pulmonary surfactants. From the depression in transition temperature of

dx.doi.org/10.1021/jp304412p | J. Phys. Chem. B 2012, 116, 9999–10007

PC vesicles, we calculated partition coefficients for PFBS; these values were 2 orders of magnitude less than PFOS or PFOA. Furthermore, PFBS disrupted the cooperativity of model PC bilayers and reduced the maximum surface pressure achieved by PC monolayers; these effects indicate a potential inhibitory effect of PFBS on pulmonary surfactant. However, the PFBS concentrations required for disruption of lipid assemblies are several orders of magnitude higher than PFOS due to differences in the bulk water-to-lipid and air−water interface partitioning. Thus PFBS is less likely to exhibit the same adverse health effects as PFOS, albeit at much higher concentrations.

AUTHOR INFORMATION

Corresponding Author

*Address: The University of Iowa, Department of Occupational and Environmental Health, University of Iowa Research Park, #221 IREH, Iowa City, IA 52242-5000. Phone: (319) 335-4310; Fax: (319) 335-4290; e-mail: hans-joachim-lehmler@uiowa.edu.

Notes

The authors declare no competing financial interest.

ACKNOWLEDGMENTS

This work was supported by the National Science Foundation (CBET-0967381/0967390), the U.S. Department of Agriculture Biomass Research and Development Initiative (Grant Agreement 68-3A75-7-608), and Grants ES005605 and ES0013661 from the National Institute of Environmental Health Sciences/National Institutes of Health.

REFERENCES

(1) Lehmler, H.-J. *Chemosphere* **2005**, *58*, 1471.
(2) U.S. EPA. *The Science of Organofluorine Chemistry*; Report AR-226-0547; U.S. EPA.: Washington, D.C., 1999.
(3) Plumlee, M. H.; McNeill, K.; Reinhard, M. *Environ. Sci. Technol.* **2009**, *43*, 3662.
(4) Xie, W.; Wu, Q.; Kania-Korwel, I.; Tharappel, J. C.; Telu, S.; Coleman, M. C.; Glauert, H. P.; Kannan, K.; Mariappan, S. V. S.; Spitz, D. R.; Weydert, J.; Lehmler, H. J. *Arch. Toxicol.* **2009**, *83*, 909.
(5) Taniyasu, S.; Kannan, K.; So, M. K.; Gulkowska, A.; Sinclair, E.; Okazawa, T.; Yamashita, N. *J. Chromatogr., A* **2005**, *1093*, 89.
(6) Naile, J. E.; Khim, J. S.; Wang, T.; Chen, C.; Luo, W.; Kwon, B.-O.; Park, J.; Koh, C.-H.; Jones, P. D.; Lu, Y.; Giesy, J. P. *Environ. Pollut.* **2010**, *158*, 1237.
(7) Taniyasu, S.; Kannan, K.; Horii, Y.; Hanari, N.; Yamashita, N. *Environ. Sci. Technol.* **2003**, *37*, 2634.
(8) Ehresman, D. J.; Froehlich, J. W.; Olsen, G. W.; Chang, S. C.; Butenhoff, J. L. *Environ. Res.* **2007**, *103*, 176.
(9) Perez, F.; Llorca, M.; Farre, M.; Barcelo, D. *Anal. Bioanal. Chem.* **2012**, *402*, 2369.
(10) Yeung, L. W. Y.; So, M. K.; Jiang, G. B.; Taniyasu, S.; Yamashita, N.; Song, M. Y.; Wu, Y. N.; Li, J. G.; Giesy, J. P.; Guruge, K. S.; Lam, P. K. S. *Environ. Sci. Technol.* **2006**, *40*, 715.
(11) Lau, C.; Anitole, K.; Hodes, C.; Lai, D.; Pfahles-Hutchens, A.; Seed, J. *Toxicol. Sci.* **2007**, *99*, 366.
(12) Lau, C.; Butenhoff, J. L.; Rogers, J. M. *Toxicol. Appl. Pharmacol.* **2004**, *198*, 231.
(13) Berthiaume, J.; Wallace, K. B. *Toxicol. Lett.* **2002**, *129*, 23.
(14) Sohlenius, A.-K.; Eriksson, A. M.; Högström, C.; Kimland, M.; DePierre, J. W. *Pharmacol. Toxicol.* **1993**, *72*, 90.
(15) Xie, W.; Bothun, G. D.; Lehmler, H. J. *Chem. Phys. Lipids* **2010**, *163*, 300.
(16) Xie, W.; Kania-Korwel, I.; Bummer, P. M.; Lehmler, H. J. *Biochim. Biophys. Acta* **2007**, *1768*, 1299.
(17) Xie, W.; Ludewig, G.; Wang, K.; Lehmler, H. J. *Colloids Surf., B* **2010**, *76*, 128.
(18) Inoue, T.; Iwanaga, T.; Fukushima, K.; Shimozawa, R.; Suezaki, Y. *Chem. Phys. Lipids* **1988**, *48*, 189.
(19) Inoue, T.; Miyakawa, K.; Shimozawa, R. *Chem. Phys. Lipids* **1986**, *42*, 261.
(20) Renner, R. *Environ. Sci. Technol.* **2006**, *40*, 12.
(21) Olsen, G. W.; Chang, S.-C.; Noker, P. E.; Gorman, G. S.; Ehresman, D. J.; Lieder, P. H.; Butenhoff, J. L. *Toxicology* **2009**, *256*, 65.
(22) Slotkin, T. A.; MacKillop, E. A.; Melnick, R. L.; Thayer, K. A.; Seidler, F. J. *Environ. Health Perspect.* **2008**, 116.
(23) Hu, W.; Jones, P. D.; Upham, B. L.; Trosko, J. E.; Lau, C.; Giesy, J. P. *Toxicol. Sci.* **2002**, *68*, 429.
(24) Lieder, P. H.; York, R. G.; Hakes, D. C.; Chang, S.-C.; Butenhoff, J. L. *Toxicology* **2009**, *259*, 33.
(25) Luebker, D. J.; Case, M. T.; York, R. G.; Moore, J. A.; Hansen, K. J.; Butenhoff, J. L. *Toxicology* **2005**, *215*, 126.
(26) Butenhoff, J. L.; Ehresman, D. J.; Chang, S.-C.; Parker, G. A.; Stump, D. G. *Reprod. Toxicol.* **2009**, *27*, 319.
(27) U.S. EPA. *Extent and Route of Excretion and Tissue Distribution of Total Carbon-14 in Rats after a Single Intravenous Dose of Fc-95-^{14}c*; Rep. AR-226-006; U.S. EPA: Washington, D.C., 1979.
(28) U.S. EPA. *A Pharmacokinetic Study of Potassium Perfluorooctanesulfonate in the Cynomolgus Monkey.*; Rep. AR226-1356; U.S. EPA: Washington, D.C., 2003.
(29) Olsen, G. W.; Burris, J. M.; Ehresman, D. J.; Froehlich, J. W.; Seacat, A. M.; Butenhoff, J. L.; Zobel, L. R. *Environ. Health Perspect.* **2007**, *115*, 1298−1305.
(30) Bischel, H. N.; Macmanus-Spencer, L. A.; Zhang, C.; Luthy, R. G. *Environ. Toxicol. Chem.* **2011**, *30*, 2423.
(31) Chen, Y. M.; Guo, L. H. *Arch. Toxicol.* **2009**, *83*, 255.
(32) Jones, P. D.; Hu, W.; De Coen, W.; Newsted, J. L.; Giesy, J. P. *Environ. Toxicol. Chem.* **2003**, *22*, 2639.
(33) Bernsdorff, C.; Wolf, A.; Winter, R.; Gratton, E. *Biophys. J.* **1997**, *72*, 1264.
(34) Zhang, X. M.; Patel, A. B.; de Graaf, R. A.; Behar, K. L. *Chem. Phys. Lipids* **2004**, *127*, 113.
(35) Bothun, G. D.; Knutson, B. L.; Strobel, H. J.; Nokes, S. E. *Langmuir* **2005**, *21*, 530.
(36) Hashizaki, K.; Taguchi, H.; Itoh, C.; Sakai, H.; Abe, M.; Saito, Y.; Ogawa, N. *Chem. Pharm. Bull.* **2005**, *53*, 27.
(37) Mabrey, S.; Sturtevant, J. M. *Proc. Natl. Acad. Sci. U.S.A.* **1976**, *73*, 3862.
(38) Kaiser, R. D.; London, E. *Biochemistry* **1998**, *37*, 8180.
(39) Aroti, A.; Leontidis, E.; Dubois, M.; Zemb, T. *Biophys. J.* **2007**, *93*, 1580.
(40) Nielson, D. W. *J. Appl. Physiol.* **1986**, *60*, 972.
(41) Arriaga, L. R.; Lopez-Montero, I.; Ignes-Mullol, J.; Monroy, F. *J. Phys. Chem. B* **2010**, *114*, 4509.
(42) Washino, N.; Saijo, Y.; Sasaki, S.; Kato, S.; Ban, S.; Konishi, K.; Ito, R.; Nakata, A.; Iwasaki, Y.; Saito, K.; Nakazawa, H.; Kishi, R. *Environ. Health Perspect.* **2009**, *117*, 660.
(43) Kamaya, H.; Kaneshina, S.; Ueda, I. *Biochim. Biophys. Acta* **1981**, *646*, 135.
(44) Custódio, J. A.; Almeida, L. M.; Madeira, V. M. C. *Biochim. Biophys. Acta* **1993**, *1153*, 308.
(45) Moya-Quiles, M. R.; Munoz-Delgado, E.; Vidal, C. J. *Chem. Phys. Lipids* **1996**, *79*, 21.
(46) Hu, W.; Jones, P. D.; DeCoen, W.; King, L.; Fraker, P.; Newsted, J.; Giesy, J. P. *Comp. Biochem. Physiol., C: Comp. Pharmacol. Toxicol.* **2003**, *135*, 77.
(47) Lohner, K. *Chem. Phys. Lipids* **1991**, *57*, 341.
(48) Matyszewska, D.; Tappura, K.; Oradd, G.; Bilewicz, R. *J. Phys. Chem. B* **2007**, *111*, 9908.
(49) Ellena, J. F.; Obraztsov, V. V.; Cumbea, V. L.; Woods, C. M.; Cafiso, D. S. *J. Med. Chem.* **2002**, *45*, 5534.
(50) van Osdol, W. W.; Ye, Q.; Johnson, M. L.; Biltonen, R. L. *Biophys. J.* **1992**, *63*, 1011.

(51) Jorgensen, K.; Ipsen, J. H.; Mouritsen, O. G.; Bennett, D.; Zuckermann, M. J. *Biochim. Biophys. Acta* **1991**, *1067*, 241.
(52) Biltonen, R. L. *J. Chem. Thermodyn.* **1990**, *22*, 1.
(53) Mukerjee, P.; Yang, A. Y. S. *J. Phys. Chem.* **1976**, *80*, 1388.
(54) Era, S.; Harada, K. H.; Toyoshima, M.; Inoue, K.; Minata, M.; Saito, N.; Takigawa, T.; Shiota, K.; Koizumi, A. *Toxicology* **2009**, *256*, 42.
(55) Jensen, M. S.; Norgaard-Pedersen, B.; Toft, G.; Hougaard, D. M.; Bonde, J. P.; Cohen, A.; Thulstrup, A. M.; Ivell, R.; Anand-Ivell, R.; Lindh, C. H.; Jonsson, B. A. *Environ. Health Perspect.* **2012**, *120*, 897−903.
(56) Grasty, R. C.; Bjork, J. A.; Wallace, K. B.; Lau, C. S.; Rogers, J. M. *Birth Defects Res., Part B* **2005**, *74*, 405.
(57) Matyszewska, D.; Tappura, K.; Oradd, G.; Bilewicz, R. *J. Phys. Chem. B* **2007**, *111*, 9908.
(58) Meister, A.; Kerth, A.; Blume, A. *J. Phys. Chem. B* **2004**, *108*, 8371.
(59) Meister, A.; Kerth, A.; Blume, A. *Phys. Chem. Chem. Phys.* **2004**, *6*, 5543.
(60) Campbell, T. Y.; Vecitis, C. D.; Mader, B. T.; Hoffmann, M. R. *J. Phys. Chem. A* **2009**, *113*, 9834.